

Braking of a Body by a Soft Inflatable Shell on Impact on a Surface

R. Sh. Gimadiev*

Kazan State Power Engineering University,
ul. 2-ya Yugo-Zapadnaya 26, Kazan, 429934 Russia

Received November 25, 2015

Abstract—The results of mathematical simulation of a solid velocity damping by a soft skeleton fabric shell filled with air on impact on a hard surface are given. The equations of motion of a falling body and of the loading dynamics of membrane shells and the reinforcement rings in the fabric shell are considered together. The mathematical model and the numerical algorithm for solving the spatial problem of the dynamics of inflation of a shell with reinforcement rings are explicitly realized by the finite difference method. The boundary conditions are posed with regard to the contact of the shell elements in compression near the ring belts. The results of numerical experiments considering the interaction of the falling body with the deformable skeleton shell are discussed. The parameters influencing the process of the body braking on impact on a surface are determined.

DOI: 10.3103/S0025654417050119

Keywords: *body braking, soft skeleton shell, spatial dynamics, results of numerical experiments.*

INTRODUCTION

Inflated fabric shells are used in aviation to absorb the energy in landing operations. Therefore, the mathematical simulation of such processes is of great importance.

In the present paper, we consider the shells which belong to the class of shells with large displacements and strains and which are reinforced by skeletons. The shell structures which experience superlarge strains in loading with elongation degrees up to $\lambda = 4$ were considered in [1–3, 17, 18]. The skeleton fabric shells with elongation degrees up to $\lambda = 1.3$ attained in the exploitation are widely used in the parachute technology [4].

The methods for calculating the interaction of parachute-type skeleton shells with the environment were developed in [5–12].

The fabric shells are also used in shipbuilding for restricting the motion of goods and fastening them by inflated elements [13]. The skeleton shells also find application in the building of inflated structures, such shells were calculated in [14].

The finite strains in shells were theoretically studied in [15–19] on the basis of the Kirchhoff geometric hypothesis stating that the normal to the middle line before deformation remains normal to it after deformation.

The most closely related problems are the following ones: the inverse problem, i.e., the lifting of a weight by an inflated soft shell, was considered in [18], pp. 135–140, and the impact of a soft spherical rubber-like gas-filled shell on an absolutely hard surface was considered in [11].

1. STATEMENT OF THE PROBLEM

We model the vertical impact of a rigid body equipped with an inflated skeleton fabric shell attached to its bottom on a horizontal hard surface.

We assume that, at the moment of contact between the lower part of the shell with the horizontal surface, the velocity of the falling body is equal to V_{gr} and directed vertically downwards, see Fig. 1. The energy of the falling weight is absorbed by the deformation of the fabric shell, i.e., the pressure inside

*e-mail: gimadiev@mail.ru

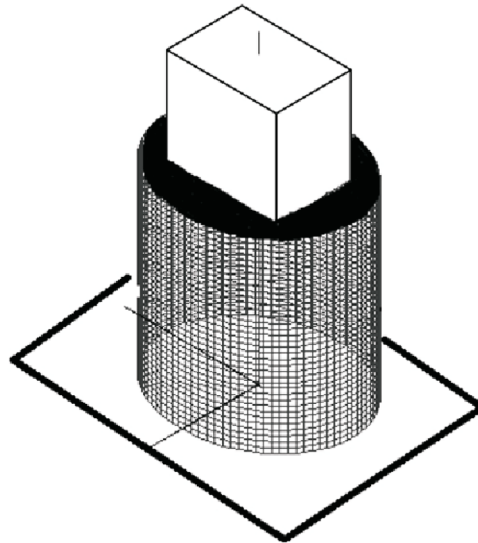


Fig. 1.

the shell which acts against the weight motion. When considering the compression of the shell, it is necessary to regard the conditions of contact between the contacting elements.

Thus, the dynamics of the shell is influenced by the conditions of contact with the falling weight, the conditions of contact with the surface, the shell structure including the conditions of contact between the shell and the ring reinforcement belts, the compression conditions, and the conditions of contact of the shell itself in the process of braking. We assume that the cargo weight is uniformly distributed over the area of the upper part of the cylindrical shell and this area remains unchanged in time. The area of the lower part of the shell adjacent to the surface also remains unchanged in the process of the shell compression due to the falling weight.

2. METHOD AND CONSTRUCTION OF THE SOLUTION

The unstrained shell Ω_0 at time $t = t_0$ under the action of external and internal forces $t > t_0$ is deformed Ω and moves in space x_γ , $\gamma = 1, 2, 3$. The shell Ω_0 is referred to curvilinear coordinates α^1, α^2, z with is normally fixed to the middle surface σ_0 .

After deformation, an arbitrary point M_0 at time t becomes $M(\alpha^i, z) \in \Omega$.

The deformed membrane shell, in cross-sections $\alpha^i = \text{const}$ and $z = \text{const}$ at time t , has thickness $h_* = h(1 + \varepsilon_3)$, where ε_3 is the true strain and λ_3 is the multiplicity of elongations in the transverse direction z .

The vector of true stresses σ^i and σ^3 is determined by the expressions

$$\sigma^i = \sigma^{ij} \mathbf{e}_j, \quad \sigma^3 = \sigma^{33} \mathbf{e}_3, \quad (2.1)$$

where σ^{ij} and σ^{33} are physical components of stresses and \mathbf{e}_j and \mathbf{e}_3 are the unit vectors on the deformed surface.

In the theory of soft shells, one considers the tensions instead of stresses, because the notion of thickness is rather conditional for fabric shells. After integration of (2.1) over the shell thickness h_* , we obtain

$$\mathbf{T}^i = T^{ij} \mathbf{e}_j, \quad \mathbf{T}^3 = T^{33} \mathbf{e}_3,$$

where $T^{ij} = h\lambda_3\sigma^{ij}$ and $T^{33} = h\lambda_3\sigma^{33}$ are physical components of tensions.

Assume that a small distinguished surface element of area $d\sigma = \sqrt{G}\partial\alpha^1\partial\alpha^2$ is under the action of surface forces p^- and p^+ applied on the sides of the surfaces $z = -h_*/2$ and $z = h_*/2$ and the mass force \mathbf{Q} , which are determined by the expressions

$$\mathbf{p} = p\mathbf{e}_3 d\sigma = p\mathbf{e}_3\sqrt{G}\partial\alpha^1\partial\alpha^2, \quad \mathbf{Q} = \mathbf{g}\rho h_* dF = \mathbf{g}h_*\rho\sqrt{G}\partial\alpha^1\partial\alpha^2,$$

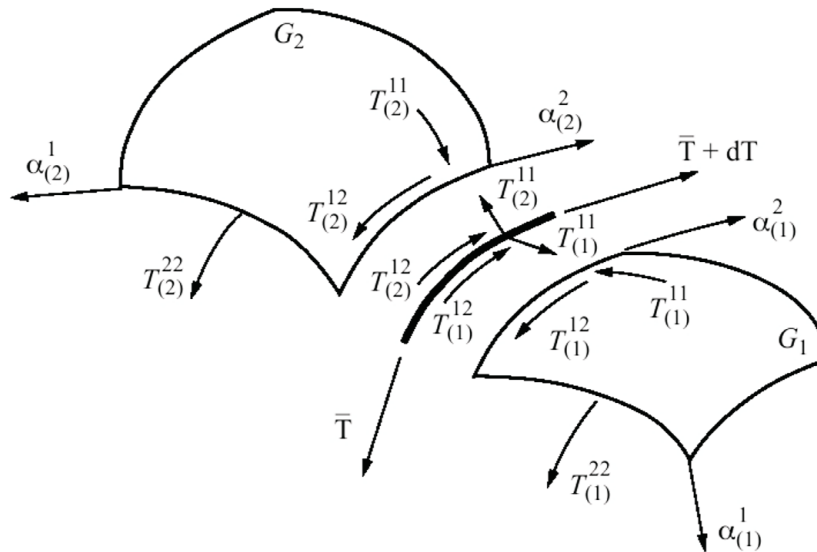


Fig. 2.

where $p = p^+ - p^-$ is the excess pressure acting on the shell and referred to the unit area σ , ρ is the density of the shell material, which does not change in the process of deformation because the shell material is assumed to be incompressible, and \mathbf{g} is the free fall acceleration.

In the membrane shell theory, the transverse force is assumed to be $T^{33} = 0$ [2], which permits assuming that the formed stress strain state (SSS) of the shell is plane stressed. Applying internal, external, and inertial forces to the distinguished shell element and following the d’Alambert principle, we obtain the equation of motion of the form

$$\rho h_* \sqrt{G} \frac{\partial^2 \mathbf{r}}{\partial t^2} = \frac{\partial}{\partial \alpha_1} [(T^{11} \mathbf{e}_1 + T^{12} \mathbf{e}_2) \sqrt{G_{22}}] + \frac{\partial}{\partial \alpha_2} [(T^{22} \mathbf{e}_2 + T^{21} \mathbf{e}_1) \sqrt{G_{11}}] + (\mathbf{p} + \rho h_* \mathbf{g}) \sqrt{G}, \quad (2.2)$$

where the unknowns are the vector function \mathbf{r} and the components of the true internal forces T^{ij} .

We consider the common deformation of a smooth shell and an element of the shell reinforcement, see Fig. 2. Assume that an absolutely flexible homogeneous filament of linear density ρ_s moves in space x_γ , $\gamma = 1, 2, 3$, under the action of a normal load of intensity \mathbf{F}_n and a tangential load of intensity \mathbf{F}_τ . The filament deformation is characterized by the elongation degree $\lambda = ds/ds_0$ or the relative elongation $\varepsilon = \lambda - 1$. The dependence of the elongation on the strain is assumed to be $\mathbf{T} = \mathbf{T}(\lambda)$ for $\lambda > 0$ and $\mathbf{T} = 0$ for $\lambda \leq 0$. The mass of the filament element before and after deformation remains the same: $dm = \rho_0 ds_0 = \rho_s ds$.

The equation of motion of an element of the elastic heavy filament in the field of gravity has the form [9]

$$\rho_0 \frac{\partial^2 \mathbf{r}}{\partial t^2} = \frac{\partial \mathbf{T}}{\partial s_0} + \mathbf{F}_n \lambda + \mathbf{F}_\tau \lambda + \mathbf{g} \rho_0, \quad (2.3)$$

where $\mathbf{r}(s_0, t)$ is the radius vector of an arbitrary point of the filament element.

Let us consider the system of Eqs. (2.2) and (2.3). Assume that the shell reinforcement element lies on one of the Lagrangian coordinates of the shell (for example, α^2). The reinforcement element has a great rigidity and separates the shell into two subregions G_1 and G_2 , see Fig. 2. Assume that, on the boundaries of these subregions of contact, on the reinforcement element, the tangential $T_{(1)}^{12}$, $T_{(2)}^{12}$ and normal $T_{(1)}^{11}$, $T_{(2)}^{11}$ tensions are realized, where the subscripts indicate the subregions G_1 and G_2 . Then the equations of motion of each subregion are described by formula (2.2) with the respective boundary tensions $T_{(1)}^{12}$, $T_{(1)}^{11}$ and $T_{(2)}^{12}$, $T_{(2)}^{11}$ for these subregions. And the vectors \mathbf{F}_n and \mathbf{F}_τ contained in the equation of motion of the shell reinforcement element (2.2) are determined in terms of the tensions $T_{(1)}^{12}$, $T_{(1)}^{11}$ and $T_{(2)}^{12}$, $T_{(2)}^{11}$ and the external loads p_l acting on the reinforcement element. Thus, we consider equations of motion of smooth shells and reinforcement elements with regard to the boundary

conditions. We note that, in the case without reinforcement elements, the shell motion is determined only by Eq. (2.2).

The cutting height of the shell is l_1 . The coordinate α_1 varies in the range $0 \leq \alpha_1 \leq l_1$, and the coordinate α_2 , in the range $0 \leq \alpha_2 \leq l_2$.

The initial conditions for the shell are $\mathbf{r}(\alpha_1, \alpha_2, t_0) = \mathbf{r}_0(\alpha_1, \alpha_2)$.

The boundary conditions of the problem are the following ones. The upper and lower covers are assumed to be absolutely rigid. The cargo weight is uniformly distributed through the upper cover along the line $\alpha_2 = l_2$. For $t \geq t_0$, we have for the upper and lower covers:

$$\mathbf{r}(0, \alpha_2, t) = \mathbf{r}_0(0, \alpha_2), \quad \mathbf{r}(l_1, \alpha_2, t) = \mathbf{r}_0(l_1, \alpha_2).$$

The equation of motion of the cargo of mass m_{gr} is assumed to be

$$m_{\text{gr}} \frac{d\mathbf{V}_{\text{gr}}}{dt} = (\mathbf{P}_1 - \mathbf{P}_0) \pi r_k^2 - m_{\text{gr}} \mathbf{g} - 2\pi r_k T_{11}(0, a_2, t) \mathbf{e}_1 \cos \gamma, \quad (2.4)$$

where \mathbf{P}_1 is the vector of pressure inside the shell, \mathbf{P}_0 is the atmospheric pressure, \mathbf{g} is the free fall acceleration, and γ is the angle between the direction of the action of the shell tension T_{11} at the point of connection of the upper cover with the radius r_k and the direction of the vector of the weight motion velocity.

We assume that the impact contact surface is smooth. In the case of a different surface configuration, it is necessary to introduce additional conditions on the boundary of contact between surface and the soft shell.

The natural boundary conditions in the shell compression are the conditions of contact between the shell elements along the reinforcement ring belts.

In numerical simulation of a soft shell in the process of oscillatory motion, due to different velocities of elements, one can observe mutually intersecting regions in the computations. The soft shells can contact but do not admit mutual intersection. Therefore, it is necessary to supplement the computational algorithm with the conditions taken into account. Such conditions will be called the *contact conditions*.

Assume that two curvilinear smooth surfaces G_1 and G_2 (Fig. 3) contact with the shell elements at points M_1 and M_2 . The curve M_1N_1 belongs to the surface G_1 , and the curve M_2N_2 belongs to the surface G_2 . The variation parameters along these curves are the arc lengths s_1 and s_2 . The current coordinates α_1 and α_2 are functions of s_1 , i.e., $\alpha_1 = \alpha_1(s_1)$ and $\alpha_2 = \alpha_2(s_1)$. Assume that the length of arc M_1N_1 is equal to Δs_1 , and point P_1 is the foot of the perpendicular dropped from point N_1 to the tangent plane passing through point M_1 . At point M_1 , we construct the unit vector \mathbf{m}_1 directed along the normal to the surface G_1 . The vector $\mathbf{P}_1\mathbf{N}_1$ is parallel to the vector \mathbf{m}_1 and then $\mathbf{P}_1\mathbf{N}_1 = \delta_1\mathbf{m}_1$, where the coefficient δ_1 is positive if the deviation $\mathbf{P}_1\mathbf{N}_1$ from the tangent plane is directed towards the vector \mathbf{m}_1 , and it is negative otherwise. Similarly, we obtain $\mathbf{P}_2\mathbf{N}_2 = \delta_2\mathbf{m}_2$ for the surface G_2 passing through point M_2 .

It is known from the differential geometry that, for infinitely small displacement of point N_1 from point M_1 , the distance P_1N_1 is equal to half the second quadratic form of the surface G_1 , i.e., $\delta_1 = I_{2,G_1}/2$, and the distance between points P_2 and N_2 is respectively equal to $\delta_2 = I_{2,G_2}/2$.

Therefore, if points M_1 and M_2 on the surfaces G_1 and G_2 contact each other, then, for an infinitely small displacement of points N_1 and N_2 on these surface along the lines s_1 and s_2 , to prevent the contact between the shell elements, it is necessary that the deviations P_1N_1 and P_2N_2 be positive:

$$\delta_1 > 0, \quad \delta_2 > 0. \quad (2.5)$$

The second quadratic form is determined by the expression [16]

$$I_{2,G} = b_{11} d\alpha_1^2 + 2b_{12} d\alpha_1 d\alpha_2 + b_{22} d\alpha_2^2, \\ b_{11} = \mathbf{m}\mathbf{r}_{11}, \quad b_{12} = \mathbf{m}\mathbf{r}_{12}, \quad b_{22} = \mathbf{m}\mathbf{r}_{22}, \quad \mathbf{r}_{ik} = \frac{\partial^2 \mathbf{r}}{\partial \alpha_i \partial \alpha_k}.$$

Thus, it is necessary to supplement the algorithm for calculating the dynamics of a soft skeleton shell with reinforcements with an analysis of the contact conditions for points belonging to different subregions, i.e., expressions of the form (2.5).

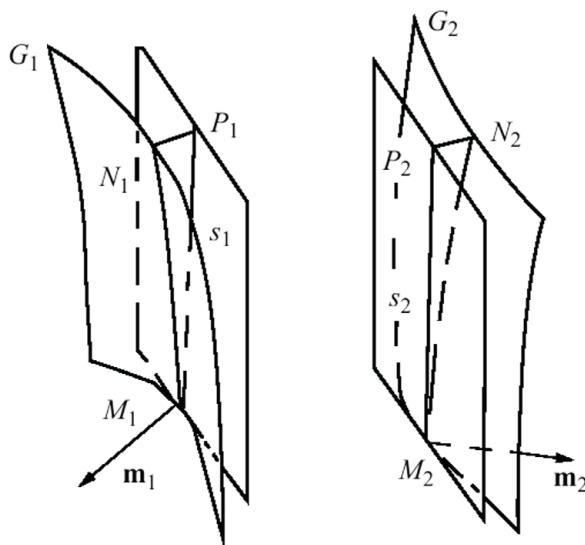


Fig. 3.

In what follows, for (2.2) instead of three unknown functions of displacements $u^\gamma(\alpha^1, \alpha^2, t)$, we consider new unknown variables representing \mathbf{r} as

$$\mathbf{r} = \mathbf{r}(\alpha^1, \alpha^2, t) = \sum_{\gamma=1}^3 x_\gamma \mathbf{i}_\gamma = x_\gamma \mathbf{i}_\gamma, \quad x_\gamma = x_\gamma(\alpha^1, \alpha^2, t),$$

where x_γ are new unknowns which are the coordinates of an arbitrary point on σ with respect to the fixed orthogonal Cartesian coordinates $Ox_1x_2x_3$ with unit vectors \mathbf{i}_γ . Then, the following relations determine the main basis vectors \mathbf{r}_j and the metric tensor components G_{ij} :

$$\mathbf{r}_j = \frac{\partial \mathbf{r}}{\partial \alpha^j} = x_{j,\gamma} \mathbf{i}_\gamma, \quad r_{j,\gamma} = \frac{\partial x_\gamma}{\partial \alpha^j}, \quad G_{jm} = \mathbf{r}_j \mathbf{r}_m = r_{j,k} r_{m,k}. \tag{2.6}$$

In this case,

$$\mathbf{e}_i = \frac{\mathbf{r}_i}{\sqrt{G_{ii}}} = l_{i\gamma} \mathbf{i}_\gamma, \quad l_{j\gamma} = \frac{r_{j,\gamma}}{\sqrt{G_{jj}}}, \quad \mathbf{e}_3 = \mathbf{e}_1 \times \mathbf{e}_2 \frac{\sqrt{G_{11}G_{22}}}{\sqrt{G}},$$

where $l_{\delta\gamma} = \cos(\mathbf{e}_\delta, \mathbf{i}_\gamma)$ are the direction cosines given by the expressions $l_{j\gamma} = r_{j,\gamma} / \sqrt{G_{jj}}$:

$$\begin{aligned} l_{31} &= (l_{12}l_{23} - l_{13}l_{22}) \frac{\sqrt{G_{11}G_{22}}}{\sqrt{G}}, \\ l_{32} &= (l_{13}l_{21} - l_{11}l_{23}) \frac{\sqrt{G_{11}G_{22}}}{\sqrt{G}}, \\ l_{33} &= (l_{11}l_{22} - l_{12}l_{21}) \frac{\sqrt{G_{11}G_{22}}}{\sqrt{G}}. \end{aligned} \tag{2.7}$$

Assume that the vector \mathbf{g} is directed along the axis x_3 . Then $\mathbf{g} = g\mathbf{i}_3$. We project Eq. (2.2) on the Cartesian axes and, taking relations (2.7) into account, obtain the three equations of motion

$$\begin{aligned} \rho h_* \sqrt{G} \frac{\partial^2 x_\gamma}{\partial t^2} &= \frac{\partial}{\partial \alpha^1} [(T^{11}l_{1\gamma} + T^{12}l_{2\gamma}) \sqrt{G_{22}}] \\ &+ \frac{\partial}{\partial \alpha^2} [(T^{22}l_{2\gamma} + T^{21}l_{1\gamma}) \sqrt{G_{22}}] + p_3 l_{3\gamma} \sqrt{G} (1 - \delta_{3\gamma} \rho h_* g), \\ \delta_{31} = \delta_{32} &= 0, \quad \delta_{33} = 1, \quad \gamma = 1, 2, 3. \end{aligned} \tag{2.8}$$

To close the obtained system of equations comprising the equations of motion (2.8) and the geometric and kinematic relations (2.6) and (2.7), it is necessary to composed physical relations for the shell with fabric base.

2.1. Physical Relations for the Fabric Shell

The fabric materials have small shear rigidity, approximately up to 2% compared with the extension rigidity [14]. Therefore, we can assume that the elasticity moduli are equal to $E_{12} = E_{21} = 0$. The the physical relations for the fabric with regard to Eqs. (2.8) can be written as [8, 14]

$$\begin{aligned} T_{11} &= \frac{E_{11}e_{11} + \nu_{21}E_{22}e_{22}}{1 - \nu_{12}\nu_{21}} + \eta\dot{e}_{11}, \\ T_{22} &= \frac{E_{22}e_{22} + \nu_{12}E_{11}e_{11}}{1 - \nu_{12}\nu_{21}} + \eta\dot{e}_{22}, \end{aligned} \tag{2.9}$$

where $\nu_{12} = \nu_{21} = 0.25$ are analogs of Poisson’s ratio, e_{11} and e_{22} are relative elongations, \dot{e}_{11} and \dot{e}_{22} are rates of relative elongations, η is the coefficient of viscous friction in the material, and E_{11} and E_{22} are extension elasticity moduli.

We write the physical relation for the ring belt in the form

$$N_{22} = \frac{E_2e_2/\Delta l + \nu_{12}E_{11}e_{11}}{1 - \nu_{12}\nu_{21}} + \eta\dot{e}_2,$$

where e_2 and E_2 are the relative elongation and the elasticity modulus for the ring skeleton, and Δl is a certain reduced width for the consistent deformation of the skeleton and the fabric.

2.2. Determination of the Excess Pressure Necessary for the Full-Stop Braking

Assume that the at the moment of contact of the shell lower part with the surface, the weight velocity is equal to V_{gr} , see Fig. 1. The weight energy is equal to the sum of the potential and kinetic energies $E = mgl_1 + mV_{gr}^2/2$, where l_1 is the cutting height of the shell.

We assume that the entire energy is spent to compress the shell, i.e., to do the work $A = \tilde{P}\tilde{F}l_1$, where \tilde{P} is the average values of pressure in the compression process, and \tilde{F} is the area of the cross-section of the deformed shell. Then we have $\tilde{P} = (mgl_1 + mV_{gr}^2/2)/(\tilde{F}l_1)$. In the general case, we can assume that the pressure increases from zero to P_{max} at time \tilde{t} and then decreases to zero during the final stage of compression at time t_k ; one can assume that the time \tilde{t} corresponds to the final stage of compression. To determine P_{max} from the condition of total absorption of the energy of the falling weight and the profile of increasing and decreasing pressure, we use the mean value theorem.

According to a special case of the mean value theorem, for a continuous function $y = f(x)$ on the interval $[a, b]$, we have $\int_a^b f(x) dx$, where $\tilde{y}(b - a)$ is the mean value of the function at an intermediate point on the interval $[a, b]$. We use this theorem to formulate the following assertion.

For two sinusoidal curves defined on the intervals $[a, \tilde{x}]$ and $[\tilde{x}, b]$, equal to zero on the boundaries of the total interval, and equal to $y_{max} = f(\tilde{x})$ at the common point, independently of the location of the point \tilde{x} on the interval $[a, b]$, the condition $y_{max} = (\pi/2)\tilde{y}$ holds, where \tilde{y} is the mean value of the function on the interval.

Indeed, if the the ascending and descending parts of the curves are sinusoids, then the area of the curvilinear trapezoid is given by the integral

$$I = y_{max} \int_a^{\tilde{x}} \sin\left(\frac{\pi}{2} \frac{x - a}{\tilde{x} - a}\right) dx + y_{max} \int_{\tilde{x}}^b \cos\left(\frac{\pi}{2} \frac{x - \tilde{x}}{b - \tilde{x}}\right) dx.$$

For the first integral, we obtain $I_1 = (2\pi)y_{max}(\tilde{x} - a)$, and for the second, $I_2 = (2/\pi)y_{max}(b - \tilde{x})$. Thus, we have $I = I_1 + I_2 = (2/\pi)y_{max}(b - a) = \tilde{y}(b - a)$, the result of integration is independent of the location of the point \tilde{x} inside the interval $[a, b]$ and $\tilde{y} = (2/\pi)y_{max}$, and hence $y_{max} = (\pi/2)\tilde{y}$.

Assume that the first phase of the shell compression takes time from $t = t_0$ to \tilde{t} , i.e., to the moment of action of the maximal pressure P_{\max} , and the second phase takes time from \tilde{t} to t_k .

Then we can assume that the law of pressure variation on the ascending and descending parts has the form

$$\tilde{p}(t) = P_{\max} \sin\left(\frac{\pi}{2} \frac{t - t_0}{\tilde{t} - t_0}\right), \quad \tilde{p}(t) = P_{\max} \cos\left(\frac{\pi}{2} \frac{t - \tilde{t}}{t_k - \tilde{t}}\right). \quad (2.10)$$

Let us determine the time t_k of the end of the shell compression in the first approximation. The mean value of the pressure in the shell during the compression \tilde{P} implies the mean value of the weight braking acceleration $\tilde{g}_p = \tilde{P}\tilde{F}/m$. In this case, the velocity of the body at the end of the shell compression is equal to $V_{\text{gr}} = V_0 + (g - \tilde{g}_p)(t_k - t_0)$, where V_0 is the weight velocity at time $t = t_0$. If the shell completely absorbs the energy of the falling body, then $V_{\text{gr}} = 0$ and thus $t_k - t_0 = V_0/(\tilde{g}_p - g)$, where $\tilde{g}_p > g$.

In the shell compression, the high-frequency vibrations of the its elements are realized, and the shell vibrations influence the value of the acting pressure. As a shell element moves against the action of internal pressure, the pressure acting on this element increases, and if it moves in the opposite direction, then this pressure decreases, i.e., the inflation is damped by the proper vibrations of the shell.

When solving the problem of the shell compression, the excess pressure $p(t)$ is approximated by the dependence

$$p(t) = \tilde{p}(t)(1 - \nu^n V^n)^2 \text{sign}(1 - \nu^n V^n), \quad (2.11)$$

which is used in the theory of soft shells to study the parachute dynamics [8]. We introduced the term $\nu^n V^n$ into formula (2.11), where ν^n is the coefficient of aerodynamic damping of the medium when a shell moves in it with the velocity $V^n = \partial u_3 / \partial t$ in the direction of normal \mathbf{e}_3 to the surface σ . Here the component u_3 of the displacement vector is calculated by the formula $u_3 = \mathbf{u}\mathbf{e}_3$.

In this dependence, the law of the excess pressure distribution \tilde{p} over the spatial coordinates α^1 and α^2 is assumed to be given (2.10) at time t .

In what follows, we assume that, for $t = t_0$, the initial shape of the shell is described by the equation $r(\alpha^1, \alpha^2, t_0) = r(\alpha^1, \alpha^2)$, where α^1 is the curvilinear coordinate along the shell generatrix varying in the range $0 \leq \alpha^1 \leq l_1$, and the circular coordinate α^2 varies in the range $0 \leq \alpha^2 \leq l_2$. The velocities of the shell elements at the initial moment are assumed to be equal to the weight velocity $dr(\alpha^1, \alpha^2, t_0)/dt = V_{\text{gr}}$, and the velocities of elements in the lower part of the shell at the moment of contact with the surface are equal to zero, $dr(l_1, \alpha^2, t)/dt$.

3. Difference Scheme for Solving the Problem

We consider an element (i, j) of the difference grid on the deformed surface and assume that its mass is concentrated at the node (i, j) .

At each time, we calculate the elongation multiplicities in the directions α^1 and α^2 by the formulas

$$\lambda_1^{i+1/2, j} = h_1^{-1} \left[\sum_{k=1}^3 (x_{i+1, j}^\gamma - x_{i, j}^\gamma)^2 \right]^{1/2}, \quad \lambda_2^{i, j+1/2} = h_2^{-1} \left[\sum_{k=1}^3 (x_{i, j+1}^\gamma - x_{i, j}^\gamma)^2 \right]^{1/2},$$

$$\lambda_1^{i+1/2, j+1/2} = \frac{\lambda_1^{i+1/2, j+1} + \lambda_1^{i+1/2, j}}{2}, \quad \lambda_2^{i+1/2, j+1/2} = \frac{\lambda_2^{i+1, j+1/2} + \lambda_2^{i, j+1/2}}{2},$$

where $h_1 = h_1(i, j)$ and $h_2 = h_2(i, j)$ are the distanced between the points $(i + 1/2, j)$, $(i, j + 1/2)$, and (i, j) of the grid.

To calculate the direction cosines of the main basis vectors, we use the relations

$$\{l_{1, \gamma}\}_j^i = \frac{x_{i+1, j}^\gamma - x_{i, j}^\gamma}{h_1 \lambda_1^{i+1/2, j}}, \quad \{l_{2, \gamma}\}_i^j = \frac{x_{i, j+1}^\gamma - x_{i, j}^\gamma}{h_2 \lambda_2^{i, j+1/2}}.$$

The equations of motion (2.2), which admit a generalized representation for the velocity vector components (here A and B are constants)

$$\frac{\partial \mathbf{V}}{\partial t} - A \frac{\partial \mathbf{T}}{\partial s} = B, \quad (3.1)$$

are associated with their difference analogs. For example, for

$$2 \leq i \leq n_1 - 1, \quad 2 \leq j \leq n_2 - 1$$

we have

$$\begin{aligned} \{V^\gamma\}^{n+1/2} &= \{V^\gamma\}^{n-1/2} + P_{i,j} \frac{\Delta t}{h_1 h_2} F_{i,j}^\gamma \\ &+ \frac{\Delta t}{\rho h_*} \left\{ \sum_{\pm} \frac{1}{2h_1} \left[\{T^{11} \lambda_2\}_{j\pm 1/2}^{i+1/2} \{l_{1\gamma}\}_{j\pm 1/2}^{i+1/2} - \{T^{11} \lambda_2\}_{j\pm 1/2}^{i-1/2} \{l_{1\gamma}\}_{j\pm 1/2}^{i-1/2} \right. \right. \\ &\quad \left. \left. + \{T^{12} \lambda_2\}_{i+1/2}^{j\pm 1/2} \{l_{2\gamma}\}_{i+1/2}^{j\pm 1/2} - \{T^{12} \lambda_2\}_{i-1/2}^{j\pm 1/2} \{l_{2\gamma}\}_{i-1/2}^{j\pm 1/2} \right] \right. \\ &\quad \left. + \sum_{\pm} \frac{1}{2h_2} \left[\{T^{22} \lambda_1\}_{i\pm 1/2}^{j+1/2} \{l_{2\gamma}\}_{i\pm 1/2}^{j+1/2} - \{T^{11} \lambda_2\}_{i\pm 1/2}^{j-1/2} \{l_{1\gamma}\}_{i\pm 1/2}^{j-1/2} \right. \right. \\ &\quad \left. \left. + \{T^{21} \lambda_1\}_{j+1/2}^{i\pm 1/2} \{l_{2\gamma}\}_{j+1/2}^{i\pm 1/2} - \{T^{21} \lambda_1\}_{j-1/2}^{i\pm 1/2} \{l_{2\gamma}\}_{j-1/2}^{i\pm 1/2} \right] - \rho h_* \delta_{3\gamma} g \right\}, \end{aligned} \quad (3.2)$$

Here

$$\{l_{1\gamma}\}_{j-1/2}^{i+1/2} = \frac{x_{i+1,g-1/2}^\gamma - x_{i,j-1/2}^\gamma}{h_1 \lambda_{i+1/2,j-1/2}^1}$$

and $F_{i,j}^\gamma$ is the sum of projections of the areas of eight triangles adjacent to the node (i, j) on the plane $x^\gamma = 0$ ($\gamma = 1, 2, 3$). So for the first triangle, we have

$$F_{i,j}^1 = \frac{1}{2} \left[x_{i,j}^2 (x_{i+1/2,j}^3 - x_{i+1/2,j+1/2}^3) + x_{i+1/2,j}^2 (x_{i+1/2,j+1/2}^3 - x_{i,j}^3) + x_{i+1/2,j+1/2}^2 (x_{i,j}^3 - x_{i+1/2,j}^3) \right].$$

The projections of the area on the other planes $x^2 = 0$ and $x^3 = 0$ are determined similarly. In this case, the indices 1, 2, 3 are changed by cyclic permutation.

The integration step is chosen according to the Courant–Friedrichs–Lewy criterion

$$\Delta t < \frac{\alpha_k \min(h_1, h_2)}{c}, \quad (3.3)$$

where α_k is the Courant coefficient and c is the speed of small perturbation propagation in the material (speed of sound).

The boundary conditions for the shell are satisfied on the expanded grid whose dimensions are determined by the numbers 1, n_1 and 1, n_2 . The indices i and j then vary in the ranges $1 \leq i \leq n_1$ and $1 \leq j \leq n_2$. The sought coordinates of the shell nodes on the time layers are determined by the formulas

$$(x^\gamma)_{i,j}^{n+1} = (x^\gamma)_{i,j}^{n+1} + \Delta t (\tilde{V}^\gamma)_{i,j}^{n+1/2} \quad (\gamma = 1, 2, 3). \quad (3.4)$$

Thus, the construction of the numerical solution of the above-formulated problem is based on the explicit scheme of the finite difference method. As a result, to construct the solution of the composed system of equations, we introduce the discrete domain

$$S_{n_i} = n_i h_j, \quad n_i = 1, 2, 3, \dots, S_i / \Delta s_i, \quad t_n = n \Delta t, \quad n = 1, 2, \dots, t / \Delta t - 1.$$

In this case, the values of the desired functions at each step of integration are determined in terms of the values already known at the preceding step in the framework of the unique algorithm of through computations.

At the initial time for $n = 0$ (i.e., for $t = -\Delta t/2$), in the equations of the form (3.2), it is first necessary to introduce $(\tilde{V}^\gamma)_{i,j}^{-1/2}$ on the expanded grid. Later, for $t > 0$, these velocities are recomputed on the extended grid at each step.

The coefficient η (2.9), which takes into account the influence of the internal friction in the material on the shell dynamics, the step of integration Δt , and the spacings h_1 and h_2 of the computational grid related by the formula (3.3), is chosen by the numerical experiments.

We note that the above-presented algorithm also permits studying the static models of mechanics of shell deformation by the pseudoviscosity method.

3.1. Estimation of the Derivative Approximation Error

In Eq. (3.1), we consider the derivative $\partial T/\partial s$ with respect to the half-integer grid

$$s_{i+1/2} = \left(1 + \frac{1}{2}\right)h, \quad i = 0, 1, 2, \dots, m-1, \quad n = 0, 1, 2, \dots,$$

for fixed time t_n , $n = 0, 1, 2, \dots$. For this, expanding the function T in a Taylor series around an integer point in [8] and using the results obtained in [20], we show that the central difference in the Lagrangian coordinate on the half-integer grid approximates the derivative $\partial T/\partial s$ up to the second order of accuracy. Since the values of Δt and Δs are related linearly by (3.3), we have $\Delta t = c_1 h$, where $c_1 = \alpha_k/c$, the derivatives $\partial V/\partial t$ can also be calculated. Therefore, the central differences with respect to the half-integer grid approximate the partial derivative $\partial T/\partial s$ and $\partial V/\partial t$ in Eq. (3.1) up to the second order of accuracy.

3.2. Equations of Motion in Dimensionless Form

To represent Eq. (2.2) in dimensionless form, we introduce the following quantities: the characteristic dimension $L = l_1$ [m] which is the length of the shell generatrix; the pressure difference and the air density ρ_B [kg/m²] which are used to determine the characteristic velocity V_0 [m/s]; the characteristic force $T_0 = \rho_B V_0^2 L^2$ [N] and the characteristic mass $M_s = 2\pi r L \rho$ [kg] of the shell; the density ρ of the shell material; and the Newton parameter $A_N = \rho_B V_0^2 L^2$. The dimensional value of the acceleration g is expressed in terms of the dimensionless parameter \tilde{g} according to the dependence $g = \tilde{g} V_0^2/L$, the change of variables is carried out $t = \tau L/V_0$, where τ is the dimensionless time, and $T_{ij} = \tilde{T}_{ij} T_0/L$, $p = \tilde{p} T_B/L^2$, $\eta = \tilde{\eta} T_0/V_0$, and $\rho = \tilde{\rho} M_s/L^2$.

4. ANALYSIS OF THE RESULTS AND EXAMPLES

We assume that the shell has a cylindrical shape of diameter $d = 0.5$ m and generatrix $l_1 = 0.6$ m. A regular grid with the respective number of cells 90×36 in the the circle and generatrix directions was used in the calculations. The shell was manufactured of capron fabric with the elasticity moduli $E_{11} = E_{22} = 20$ kN/m in the the circle and generatrix directions. The fabric density was $\rho = 0.05$ kg/m². The shell was reinforced by three ring belts of five fabric layers located at a uniform spacing along the shell height. The mass of the falling weight was $G = 100$ kg. The initial velocity of the weight and the shell at the moment of contact of the cylindrical shell lower part with the surface was set to be $V_{gr} = 6.0$ m/s.

The pressure is determined by the dynamic pressure $p = k_p \rho_B V_0^2/2$, where the characteristic velocity is $V_0 = 80$ [m/s], the air density is $\rho_B = 0.125g$ [kg/m³], and the coefficient of the pressure increase is $k_p = 4$. In the calculations, it was assumed that the value of the pressure difference p in compression inside the shell remains unchanged.

The initial state corresponding to these data is shown in Fig. 1; the process of weight braking starts from this moment. Figure 4 illustrates the results of numerical experiment of the process of weight braking.

The shell maximal deformation in the circular direction occurs at time $t = 0.0025$ s in the middle of the shell, and the maximal dimensionless tensions are $T_{22} = 6.099$ at this moment. The weight velocity is equal to $V_{gr} = 6.018$ m/s, and the weight height is $H_{gr} = 0.975l_1$. At time $t = 0.052$ s, the weight velocity is equal to $V_{gr} = 5.359$ m/s, and the shell is compressed by a half, and the weight height is $H_{gr} = 0.5l_1$. At time $t = 0.101$ s, the weight velocity is equal to $V_{gr} = 4.503$ m/s, and the weight height is $H_{gr} = 0.1l_1$.

Figure 5 presents the graph of surface circular tensions for this time. The maximal dimensionless tensions $T_{22} = 1.706$ are also realized in the middle of the shell. The reinforcement belts significantly decrease the level of circular tensions.

The total braking time was equal to $t_k = 0.125$ s. And the weight velocity at the moment of contact with the surface was $V_{gr} = 4.04476$ m/s.

Let us test the program by calculations. Assume that the pressure in the shell in compression is preserved to be $p = 0$ (free fall of the body). At the initial moment of motion, the weight moves with velocity $V_{gr} = 6.0$ m/s. The time of fall from the height $l_1 = 0.6$ m is determined by the equation $gt^2 + 2V_{gr}t - 2l_1 = 0$ and is equal to $t = 0.09294$ s. And the velocity of free fall at the moment of contact

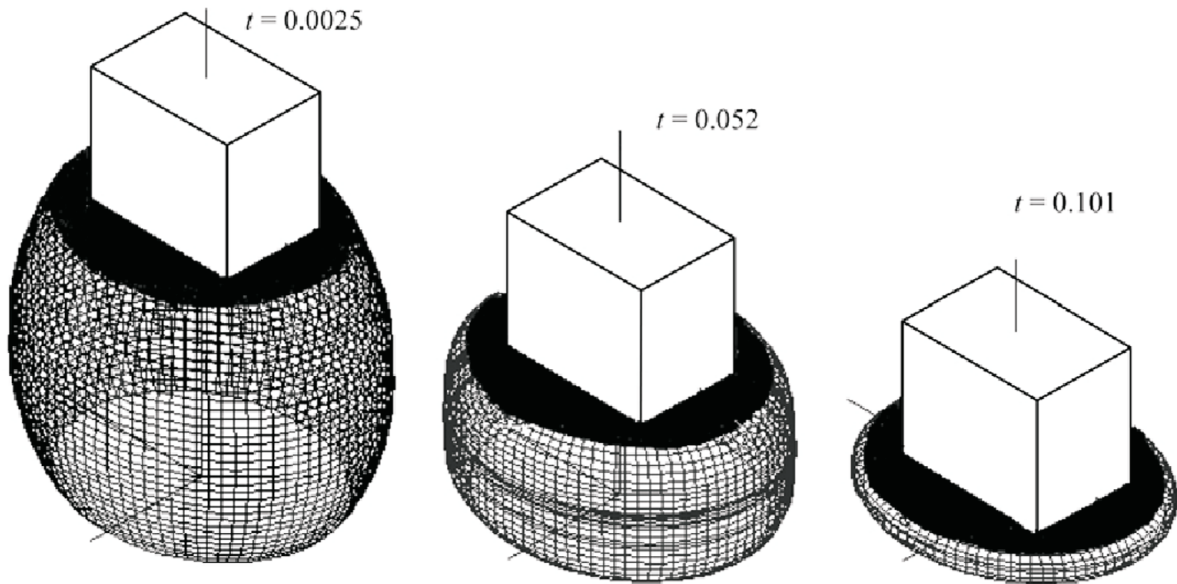


Fig. 4.

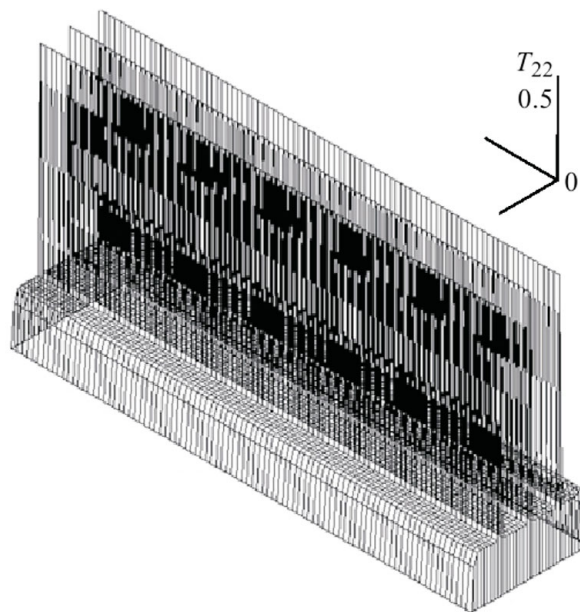


Fig. 5.

with the surface is $V_{gr} = 6.91143$ m/s. Let us consider this problem by numerical integration according to the above algorithm. We obtain $V_{gr} = 6.91003$ m/s. The relative error compared with the exact solution is $\varepsilon = 0.0203\%$. This calculation was used to choose the Courant coefficient $\alpha_k = 0.02$ in formula (3.3), which ensures the stability of the solution.

The use of the inflated soft shell allows us in the computational case to decrease the weight velocity on impact on the surface by $\Delta V = 6.91143 - 4.04476 = 2.86667$ m/s.

In the calculations for a fabric with elasticity moduli $E_{11} = E_{22} = 18.75$ kN/m, the body velocity on impact on the surface was equal to $V_{gr} = 3.88157$ m/s. And the computations for $E_{11} = E_{22} = 15$ kN/m give the velocity $V_{gr} = 3.76559$ m/s.

Thus, decreasing the modulus of elasticity of the material (i.e., using a more deformable materials),

one can decrease the body velocity on impact on the surface. This effect occurs due to a greater deformation of the shell and an increase in the effective area of pressure acting against the weight motion. The velocity of fall also decreases because of an increase in the pressure inside the shell.

5. CONCLUSION

A mathematical model of braking a falling weight by a soft skeleton shell inside which the pressure acts against the weight motion at the moment of its contact with the surface.

A numerical algorithm for solving partial differential equations with boundary contact conditions for elements of the soft shell in its compression.

A numerical experiment was carried out to verify the calculation method and the parameters influencing the process of the body braking were revealed. The results of computations agree well with the general concepts of braking of a falling weight.

REFERENCES

1. A. G. Giniyatullin and R. Sh. Gimadiev "Studies of the Balloon Catheter Shell Inflation," *Med. Tekhn.*, No. 2, 30–33 (1993).
2. R. Sh. Gimadiyev, T. Z. Gimadiyeva, and V. N. Paimushin, "The Dynamic Process of the Inflation of Thin Elastomeric Shells under the Action of an Excess Pressure," *Prikl. Mat. Mekh.* **78** (2), 236–248 (2014) [*J. Appl. Math. Mech. (Engl. Transl.)* **78** (2), 163–171 (2014)].
3. R. Sh. Gimadiev, T. Z. Gimadiyeva, and V. N. Paimushin, "Mathematical Simulation of Dynamics at Elastomeric Shells Inflation," in *Int. Conference on the Methods of Aerophysical Research. 19–25 August, 2012. Kazan, Russia*, Abstracts, Vol. 1 (Kazan, 2012) pp. 114–115.
4. A. N. Lobanov, *Foundations of Parachute Calculation and Design* (Mashinostroenie, Moscow, 1965) [in Russian].
5. M. A. Il'gamov, *Introduction to Nonlinear Hydroelasticity* (Nauka, Moscow, 1991) [in Russian].
6. N. F. Morozov, A. T. Ponomarev, and O. V. Rysev, *Mathematical Modeling of Complex Aeroelastic Systems* (Fizmatlit, Moscow, 1995) [in Russian].
7. Yu. V. Moiseev, O. V. Rysev, and V. V. Fedorov, "Mathematical Model of Two-Shell Gliding Parachute Shaping," in *Proc. of the Seminar "Shell Interaction with Environment,"* No. 20 (Kazan, KFTI, KF Akad. Nauk SSSR, 1985), pp. 31–40 [in Russian].
8. R. Sh. Gimadiev, *Dynamics of Soft Parachute-Type Shells* (Kazan Gos. Energ. Univ., Kazan, 2006) [in Russian].
9. R. Sh. Gimadiev, V. P. Kurinskaya, and Yu. V. Mikhailovskii, "Numerical and Experimental Study of Ribbon Cross-Shaped Parachute Opening," *Izv. Vyssh. Uchebn. Zaved. Aviats. Tekhnika*, No. 1, 6–11 (1997).
10. V. V. Ridel and B. V. Gulin, *Dynamics of Soft Shells* (Nauka, Moscow, 1990) [in Russian].
11. A. N. Gilmanov, "Dynamics of Impact Interaction of a Soft Gas-Filled Spherical Shell with a Soft Surface." *Trudy Sem. "Nonlinear Problems of Aerohydroelasticity"* (Kazan, KFTI, KF Akad. Nauk SSSR), No. 11, 98–114 (1979).
12. R. R. Shagidullin, *Problems of Mathematical Modeling of Soft Shells* (Kazan Mat. Obshch., Kazan, 2001) [in Russian].
13. V. E. Magula, *Ship Elastic Structures* (Sudostroenie, Leningrad, 1978) [in Russian].
14. F. Otto and R. Trostel, *Pneumatic Building Structures* (Stroiizdat, Moscow, 1967) [in Russian].
15. V. V. Novozhilov, *Fundamentals of Nonlinear Elasticity* (OGIZ, Leningrad–Moscow, 1948) [in Russian].
16. K. Z. Galimov, *Foundations of Nonlinear Theory of Thin Shells* (Izdat. Kazan. Univ., Kazan, 1975) [in Russian].
17. K. F. Chernykh, *Nonlinear Elasticity in Engineering* (Mashinostroenie, Leningrad, 1986) [in Russian].
18. E. P. Kolpak, *Stability of Membrane Shells in Large Deformations* (SPbGU, St. Petersburg, 2000) [in Russian].
19. V. N. Paimushin, "A Theory of Thin Shells with Finite Displacements and Deformations Based on a Modified Kirchhoff–Love Model," *Prikl. Mat. Mekh.* **75** (5), 813–829 (2011) [*J. Appl. Math. Mech. (Engl. Transl.)* **75** (5), 568–579 (2011)].
20. A. A. Samarskii and Yu. P. Popov, *Difference Schemes for Gas Dynamics* (Nauka, Moscow, 1992) [in Russian].